# Model Energy Landscapes

**Pablo G. Debenedetti,\*,† Frank H. Stillinger,‡ and M. Scott Shell†**

*Departments of Chemical Engineering and Chemistry, Princeton University, Princeton, New Jersey 08544*

*Received: July 18, 2003; In Final Form: October 10, 2003*

The multidimensional potential-energy "landscape" formalism offers useful insights into the properties of supercooled liquids and glasses. However, its mathematical fundamentals present formidable subtlety and complexity. In the interests of developing a useful approximation for the statistical mechanics of landscapes, we have developed a simple family of models describing the energy-depth distribution of landscape basins. Our analysis begins with the "Gaussian" model that has been advocated in the recent literature, a physically appealing and thermodynamically rather accurate description that straightforwardly predicts a positive-temperature ideal glass transition. Careful enumeration of low-lying basins reveals however that the Gaussian model requires modification in the form of a logarithmic correction. Consequently, we have carried out algebraic and numerical analyses of a logarithmically modified Gaussian model, including depth dependence of the mean intrabasin vibrational free energy. The logarithmic modification has the effect of eliminating the positive-temperature ideal glass transition of the precursor pure-Gaussian model. Nevertheless, it is sufficiently similar to that unmodified model at and above any kinetic glass transition temperature to be able to represent measurable calorimetric data with reasonable accuracy.

## I. Introduction

Recent years have witnessed an explosive growth of interest in the theory of glasses (amorphous solids) and of the viscous liquids from which they are commonly formed by rapid cooling.[1−4] The technical applications of amorphous solids are numerous. Examples include the use of carbohydrate glasses to prolong the shelf life of labile biochemicals in the pharmaceutical industry;[5] optical waveguides, which consist of amorphous silica; the use of metallic glasses for corrosion resistance;[6] photovoltaic cells made of glassy silicon; engineering plastics, the majority of which are amorphous;[7] and of course window glass, which consists mainly of sand, lime, and soda and is the best-known and oldest example of an engineered amorphous solid.[8] Scientifically, viscous liquids and glasses command interest because the molecular basis underlying their physical properties and rich phenomenology remains incompletely understood. One of the distinguishing characteristics of deeply supercooled liquids near their glass transition is the pronounced slowing down of their rate of structural relaxation. A striking manifestation of this slowing down is the extraordinary increase in shear viscosity near the glass transition, by as much as 3 orders of magnitude over a temperature interval of 10 K.[9] Understanding the way in which liquids acquire amorphous rigidity upon cooling without undergoing appreciable structural change is one of the most important challenges in modern condensed matter physics.[10]

In glasses and viscous liquids, molecules are in simultaneous contact with many neighbors. Under these conditions, it is natural to consider their full *N*-body potential-energy function $\Phi(\mathbf{x}_1...\mathbf{x}_N)$ of the configurational coordinates and to seek to describe the manner in which its details generate the variety of experimentally observed collective thermodynamic and kinetic phenomena.[11] The potential energy as a function of the system's configurational degrees of freedom has frequently been called its "energy landscape", thereby suggesting novel modes of analysis. The energy landscape perspective has emerged as a useful tool for the theoretical and computational investigation of condensed-matter phenomena generally, but specifically of supercooled and glassy behavior. Some recent examples of the application of landscape-based concepts include studies of the temperature-dependent manner in which a liquid samples its potential energy landscape and its relationship to the dynamics of structural relaxation;[12] investigation of the mechanical properties of molecular fluids;[13] calculation of liquid-phase properties from the statistics governing the sampling of local potential-energy minima;[4,14] studies of the relationship between macroscopic flow and transitions between local minima in the energy landscape;[15] and analysis of the relationship between configurational entropy and diffusivity in supercooled water.[16]

Even in the simplest case of a fluid composed of structureless particles with no internal degrees of freedom, the energy landscape is a hypersurface in $3N + 1$ dimensions whose visualization is impossible for even modest system sizes *N*. Furthermore, the number of permutationally distinct local potential-energy minima has the approximate asymptotic form $\exp(KN)$, where *K* is a positive, *N*-independent quantity.[17] This exponentially huge enumeration total forces the description of landscapes to be statistical rather than taxonomic.[18] A central quantity in the statistical theory then becomes the density of potential-energy minima as a function of their depth, and the investigation of such depth distributions for various material systems is currently a very active area of research. One preferred approach is to simulate the motion of several hundred molecules by computer, either stochastically or deterministically.[12,16,19−26] Periodic energy minimizations then provide information on the manner in which the system samples its underlying energy landscape as a function of the imposed thermodynamic condi-

---

\* Author to whom correspondence may be addressed. E-mail: pdebene@princeton.edu.
† Department of Chemical Engineering.
‡ Department of Chemistry.

Model Energy Landscapes

*J. Phys. Chem. B, Vol. 107, No. 51, 2003* **14435**

tions, such as temperature and density. Although this approach has already yielded valuable information, the computational demands resulting from the need to couple conventional Monte Carlo or molecular dynamics with frequent energy minimizations are considerable, and it is important to explore simultaneously other routes to the investigation of energy landscapes in many-body systems. One such alternative approach consists of constructing model functions to describe the statistical properties of energy landscapes for real substances and to investigate theoretically the ensuing collective thermodynamic and dynamical consequences.[4] This is the strategy that we follow in this work.

In the interests of completeness and self-containment, the following section II summarizes the basic definitions and formulas that describe thermal equilibrium in the energy landscape ("inherent structure") formalism. This leads naturally to the simplest "reasonable" model for the landscape depth distribution, the Gaussian model, whose attributes and implications form the subject of section III. One of those implications is the prediction of an "ideal glass transition" at a positive "ideal glass transition temperature". Section IV focuses on the enumeration of amorphous inherent structures at the low-potential-energy end of the distribution and reaches the conclusion that the otherwise useful Gaussian distribution requires a qualitative modification; the modification has the effect, in principle, of eliminating the ideal glass transition. Section V thereupon introduces a logarithmically modified version of the Gaussian distribution. Numerical analysis of that modified form leads to results that are presented in section VI. Those numerical results include an unexpected "fixed point" phenomenon. They also illustrate the fact that calorimetric data for glass formers obtained at temperatures above an experimental (kinetically controlled) glass transition can invite simple extrapolation that misleadingly suggests a false conclusion about the existence of an ideal glass transition. The final section VII summarizes conclusions and provides discussion of several relevant issues. Throughout this work we use the term "ideal glass transition" to denote the condition in which the system adopts a mechanically stable amorphous configuration possessing the lowest available energy. The same term is sometimes used to describe the transition from ergodic to nonergodic behavior as predicted by mode-coupling theory.[27] The two phenomena are very different and should not be confused.

## II. Basic Formulas

The descriptive formalism to be used in the following has been developed to describe and to exploit the multidimensional landscape topography of $\Phi(\mathbf{x}_1...\mathbf{x}_N)$, the many-particle potential-energy function. Here the coordinates of the individual particles have been denoted by the $\mathbf{x}_i$ ($1 \leq i \leq N$); they specify center positions, spatial orientations, and molecular internal degrees of freedom, as required by the case of interest. The potential-energy function is basic to determination of both the dynamical evolution and the thermodynamic equilibrium states of the many-particle system.

By implementing a steepest-descent mapping for the function $\Phi$, it is possible to divide the multidimensional configuration space of particle coordinates exhaustively into a set of "basins", each one containing a single local $\Phi$ minimum ("inherent structure").[11] A convenient and natural-order parameter for classifying potential-energy minima of a many-body system is their depth on a per-particle basis[4,11]

$$\varphi = \Phi(\text{min})/N \qquad (\text{II.1})$$

In the conventional large-system limit (with particle-number density $\rho$ held fixed), the depth distribution $W(\varphi,\rho)$ of geometrically distinguishable potential-energy minima can legitimately be treated as a continuous and at-least-once-differentiable function of $\varphi$. In accord with the behavior of the total number of inherent structures, $W(\varphi,\rho)$ is also asymptotically an exponentially rising function of $N$. Therefore, for present purposes we simply write

$$W(\varphi,\rho) = C \exp[N\sigma(\varphi,\rho)] \qquad (\text{II.2})$$

Here, $\sigma(\varphi,\rho) \geq 0$ is independent of $N$, and $C$ is a normalization constant with dimensions (energy)$^{-1}$ that is also independent of $N$.[11] The $\varphi$ range of definition for the enumeration function $\sigma(\varphi,\rho)$ is bounded by a lower-limit $\varphi_l$, corresponding to the energetically most stable arrangement (inherent structure) of particles at number-density $\rho$ and by an upper limit $\varphi_u$, the potential energy per particle of the least-stable (highest-lying) inherent structure at that number-density $\rho$

$$\varphi_l(\rho) \leq \varphi \leq \varphi_u(\rho) \qquad (\text{II.3})$$

Because the particle arrangements at these extremes are expected to be substantially unique, aside from permutational symmetry, they should be points at which the enumeration function vanishes

$$\sigma(\varphi_l,\rho) = \sigma(\varphi_u,\rho) = 0 \qquad (\text{II.4})$$

The vast majority of the inherent structures have depth parameters lying between these extremes, the implication of which is that $\sigma(\varphi,\rho)$ should pass through a maximum with respect to $\varphi$ within the interval (II.3).

The tiling of the multidimensional configuration space by basins and the identification of their embedded potential minima leads to a separation of the many-body problem into a purely configurational part (the inherent structures) and a vibrational deformation part (the intrabasin displacements from the inherent structures). This in turn creates a formal simplification for the canonical partition function that describes the states of thermodynamic equilibrium. The result is the following expression for the Helmholtz free energy per particle that is asymptotically exact in the large-system limit[11]

$$\beta F/N = \min_{(\varphi)}[\beta\varphi - \sigma(\varphi,\rho) + \beta f^{(\text{vib})}(\varphi,\beta,\rho)]$$

$$= \beta\varphi^* - \sigma(\varphi^*,\rho) + \beta f^{(vib)}(\varphi^*,\beta,\rho) \qquad (\text{II.5})$$

Here $\beta = 1/k_BT$, where $k_B$ is Boltzmann's constant and $f^{(\text{vib})}(\varphi,\beta,\rho)$ is the vibrational free energy per particle for intrabasin displacements, averaged over basins with depths in a narrow range about $\varphi$. The quantity $\varphi^*(\beta,\rho)$ is the value of the order parameter that locates the depth of basins preferentially occupied under the prevailing temperature and density conditions; it obeys the variational relation

$$\{(\partial/\partial\varphi)_{\beta,\rho}[\sigma(\varphi,\rho) - \beta f^{(\text{vib})}(\varphi,\beta,\rho)]\}_{\varphi=\varphi^*} = \beta \quad (\text{II.6})$$

Because expression II.5 refers to strict thermal equilibrium, it automatically contains the capacity to describe the liquid above its melting temperature as well as the freezing of the liquid into the crystalline solid phase at lower temperature. However, if interest primarily lies in describing the molecular behavior of supercooled liquids and the glasses that they form, a modification of the basin/inherent structure representation must be implemented. Specifically, this requires projecting out of

consideration all basins whose inherent structures contain substantial patterns of crystallinity.[28] As a result, only those basins corresponding to amorphous inherent structures will be considered, and they possess a diminished distribution function $W_a(\varphi,\rho)$, and corresponding enumeration function $\sigma_a(\varphi,\rho)$. Furthermore, this amorphous basin set is defined over a foreshortened $\varphi$ interval

$$\varphi_l(\rho) < \varphi_{la}(\rho) \leq \varphi \leq \varphi_{ua}(\rho) \leq \varphi_u(\rho) \qquad \text{(II.7)}$$

The lower amorphous limit is expected to be above that of the most stable crystalline configuration, but it is less certain that the constraint of amorphous character has the effect of moving the upper limit downward.

After the removal of crystallite-containing basins, the resulting modified canonical partition function describes the "equilibrated" liquid below its normal freezing point. The Helmholtz free energy for the metastable supercooled liquid then possesses a representation entirely analogous to that shown in eqs II.5 and II.6 above

$$\beta F_a/N = \beta\varphi_a{}^* - \sigma_a(\varphi_a{}^*,\rho) + \beta f_a{}^{(vib)}(\varphi_a{}^*,\beta,\rho) \quad \text{(II.8)}$$

and the mean depth $\varphi_a{}^*(\beta,\rho)$ of the bottoms of the dominating amorphous-structure basins satisfies the modified variational condition

$$\{(\partial/\partial\varphi)_{\beta,\rho}[\sigma_a(\varphi,\rho) - \beta\varphi - \beta f_a{}^{(vib)}(\varphi,\beta,\rho)]\}_{\varphi=\varphi_a{}^*} = 0 \quad \text{(II.9)}$$

In these expressions, $f_a{}^{(vib)}$ is the depth-dependent vibrational free energy per particle for the restricted basin set.

The constant-volume heat capacity of the amorphous system, $C_{Va}$ follows by applying two constant-volume $\beta$ derivatives to the Helmholtz free-energy expression II.8 and applying the variational criterion (II.9)

$$\frac{C_{Va}}{Nk_B} = -\beta^2\left\{\left[1 + \left(\frac{\partial f_a{}^{(vib)}}{\partial\varphi}\right)_{\beta,\rho} + \beta\left(\frac{\partial^2 f_a{}^{(vib)}}{\partial\beta\partial\varphi}\right)_\rho\right]\left(\frac{\partial\varphi_a{}^*}{\partial\beta}\right)_\rho + \right.$$
$$\left. 2\left(\frac{\partial f_a{}^{(vib)}}{\partial\beta}\right)_{\varphi,\rho} + \beta\left(\frac{\partial^2 f_a{}^{(vib)}}{\partial\beta^2}\right)_{\varphi,\rho}\right\}_{\varphi=\varphi_a{}^*} \quad \text{(II.10)}$$

Notice that despite the clean separation of configurational and vibrational contributions to the free-energy expression II.8, this heat capacity formula exhibits cross terms (the second and third terms) between these two types of degrees of freedom. In any case, thermodynamic relations II.8–II.10 cease to have direct experimental relevance once the system is cooled below a kinetic glass transition temperature and is then unable to sustain equilibration within the manifold of amorphous-state basins.

Although the Helmholtz free energy $F_a$ has direct relevance to isochoric (constant volume) conditions, the Gibbs free energy $G_a$ is more directly connected to the isobaric (constant pressure) conditions under which the majority of laboratory studies of supercooled liquids and glasses are performed. To derive isobaric expressions analogous to those displayed in eqs II.8–II.10, one starts by replacing the potential energy $\Phi$ with a "potential enthalpy" function $\Psi$, whose variables are the set of molecular coordinates augmented with the fluctuating system volume $V$[29]

$$\Psi(\mathbf{x}_1...\mathbf{x}_N,V) = \Phi(\mathbf{x}_1...\mathbf{x}_N) + pV \qquad \text{(II.11)}$$

where $p$ is the applied pressure. The relevant configuration space is thus increased by one dimension, and in that larger space

steepest-descent mapping on the $\Psi$ hypersurface identifies isobaric basins and their embedded isobaric inherent structures. After removing crystal-pattern-containing basins, isobaric distribution, enumeration, and vibrational free-energy functions $\hat{W}_a$, $\hat{\sigma}_a$, and $\hat{f}_a{}^{(vib)}$ can be defined by straightforward extension of the isochoric case. The supercooled liquid Gibbs free-energy then follows a format analogous to that shown earlier for the Helmholtz free energy but now using the enthalpy per particle $\psi$ as the appropriate intensive order parameter

$$\beta G_a/N = \beta\psi_a{}^* - \hat{\sigma}_a(\psi_a{}^*,p) + \beta\hat{f}_a{}^{(vib)}(\psi_a{}^*,\beta,p) \quad \text{(II.12)}$$

The dominating isobaric basin depth $\psi_a{}^*$ satisfies a variational criterion analogous to that in eq II.9

$$\{(\partial/\partial\psi)_{\beta,p}[\hat{\sigma}(\psi,p) - \beta\psi - \beta\hat{f}_a{}^{(vib)}(\psi,\beta,p)]\}_{\psi=\psi_a{}^*} = 0 \quad \text{(II.13)}$$

The constant-pressure heat capacity $C_{pa}$ for the amorphous system then possesses a form analogous to that for $C_{Va}$ shown above in eq II.10 upon application of two constant-pressure $\beta$ derivatives

$$\frac{C_{pa}}{Nk_B} = -\beta^2\left\{\left[1 + \left(\frac{\partial\hat{f}_a{}^{(vib)}}{\partial\psi}\right)_{\beta,p} + \beta\left(\frac{\partial^2\hat{f}_a{}^{(vib)}}{\partial\beta\partial\psi}\right)_p\right]\left(\frac{\partial\psi_a{}^*}{\partial\beta}\right)_p + \right.$$
$$\left. 2\left(\frac{\partial\hat{f}_a{}^{(vib)}}{\partial\beta}\right)_{\psi,p} + \beta\left(\frac{\partial^2\hat{f}_a{}^{(vib)}}{\partial\beta^2}\right)_{\psi,p}\right\}_{\psi=\psi_a{}^*} \quad \text{(II.14)}$$

Although the landscape relations displayed above concern thermodynamic (i.e., static) properties of the supercooled liquid, the venerable Adam–Gibbs theory[30] offers a useful connection to time-dependent characteristics. This theory developed and exploited the concept of independent "cooperatively rearranging regions" within the liquid medium whose kinetics were postulated to underpin relaxation phenomena in the supercooled temperature range. A principal conclusion of the Adam–Gibbs approach was that long mean relaxation times $\tau$ observed for deeply supercooled liquids could be expressed in the following form

$$\tau(T) = \tau_0 \exp\left(\frac{A}{TS_{conf}(T)}\right) \qquad \text{(II.15)}$$

here $\tau_0$ and $A$ are temperature-independent constants, and $S_{conf}$ is the configurational contribution to the system entropy. The potential energy, or potential enthalpy, landscape viewpoint provides an immediate identification of that configurational entropy, having separated the vibrational contributions. Under isochoric (constant volume) circumstances

$$S_{conf}(T,\rho) = Nk_B\sigma_a[\varphi_a{}^*(T),\rho] \qquad \text{(II.16)}$$

while under isobaric (constant pressure) circumstances

$$S_{conf}(T,p) = Nk_B\hat{\sigma}_a[\psi_a{}^*(T),p] \qquad \text{(II.17)}$$

Given this interpretation, models of the inherent-structure depth distribution for the purposes of thermodynamic description automatically become models for relaxation phenomena as well and by implication for the temperature dependence of shear viscosity $\eta(T)$. This stems from the generalization of the fact that for a Maxwell fluid, $\eta$ can be written as a product of a shear relaxation time $\tau$ and a high-frequency modulus $G_\infty$, where

Model Energy Landscapes

*J. Phys. Chem. B, Vol. 107, No. 51, 2003* **14437**

the former obeys eq II.15 and the latter is only weakly dependent on temperature.

It should be noted in passing that thermodynamic measurements will access only a portion of the $\varphi_a$ or $\psi_a$ intervals over which the respective distribution functions $W_a$ or $\hat{W}_a$ are defined. Specifically, the very high potential energy, or very high potential enthalpy portions of these distributions would not contribute to thermodynamic functions. However, this does not mean that they have no physical significance. Basins for unusually high isochoric or isobaric inherent structures can certainly be populated by irreversible processes (cold working, deposition from the vapor phase, etc.). Also, formal analytic continuation of equilibrium properties from positive to negative $\beta$ (positive to negative temperature) is a process for accessing the high $\varphi$ and high $\psi$ parts of the distributions.[31]

### III. Gaussian Landscape Distribution

The simplest functional form for the basin-depth distribution functions $W_a(\varphi,\rho)$ and $\hat{W}_a(\psi,p)$ that might offer qualitatively useful representations for an amorphous landscape would be Gaussian functions of the intensive depth parameter $\varphi$ or $\psi$. In other words, the respective enumeration functions $\sigma_a(\varphi,\rho)$ and $\hat{\sigma}_a(\psi,p)$ would be approximated by inverted parabolas. Specifically, one can set

$$\sigma_a(\varphi,\rho) \cong \alpha_0(\rho) - \alpha_2(\rho)[\varphi - \varphi_0(\rho)]^2 \quad \text{(III.1)}$$

$$\hat{\sigma}_a(\psi,p) \cong \hat{\alpha}_0(p) - \hat{\alpha}_2(p)[\psi - \psi_0(p)]^2 \quad \text{(III.2)}$$

Note that all of the $\alpha$'s are positive and that $\varphi_0$ and $\psi_0$ locate the distribution maxima, respectively. The lower and upper limits of the inherent structure distributions are the points at which these quadratic functions vanish

$$\varphi_{la} = \varphi_0 - (\alpha_0/\alpha_2)^{1/2}$$
$$\varphi_{ua} = \varphi_0 + (\alpha_0/\alpha_2)^{1/2} \quad \text{(III.3)}$$
$$\psi_{la} = \psi_0 - (\hat{\alpha}_0/\hat{\alpha}_2)^{1/2}$$
$$\psi_{ua} = \psi_0 + (\hat{\alpha}_0/\hat{\alpha}_2)^{1/2} \quad \text{(III.4)}$$

The qualitative applicability of these Gaussian distribution forms receives support from approximate distributions that have been derived from experimental calorimetric data on several glass formers; these have included o-terphenyl at 1 atm[29] as well as 1-propanol and 3-methylpentane at various pressures.[31] It also receives support from atomistic simulations that directly examine inherent structures and their depth distributions in liquids.[22,32]

Thermodynamic application of the model forms (III.1 and III.2) would be straightforward if correspondingly simple expressions could be justified for the vibrational free energy quantities $f_a^{(vib)}$ and $\hat{f}_a^{(vib)}$ as functions of their respective depth variables. A natural first estimate would be that these functions are independent of their depth variables, which is equivalent to assuming that, on average, basins have the same aperture profile regardless of their position on the depth scale. While this may not be grossly inaccurate, evidence indicates that a better assumption is that these vibrational free energies have a modest linear dependence on basin depth and that the linear dependence is itself proportional to absolute temperature.[32,33] Thus we write

$$f_a^{(vib)}(\varphi,\beta,\rho) \cong f_1(\beta,\rho) + \beta^{-1}F(\rho)(\varphi - \varphi_0) \quad \text{(III.5)}$$

$$\hat{f}_a^{(vib)}(\psi,\beta,p) \cong \hat{f}_1(\beta,p) + \beta^{-1}\hat{F}(p)(\psi - \psi_0) \quad \text{(III.6)}$$

When isochoric expressions (eqs III.1 and III.5) are inserted into eq II.9 for the determination of $\varphi_a$*, the result is a linear equation with the solution

$$\varphi_a*(\beta,\rho) = \varphi_0(\rho) - \frac{\beta + F(\rho)}{2\alpha_2(\rho)} \quad \text{(III.7)}$$

An analogous result describes the isobaric case

$$\psi_a*(\beta,p) = \psi_0(p) - \frac{\beta + \hat{F}(p)}{2\hat{\alpha}_2(p)} \quad \text{(III.8)}$$

The last two expressions, eqs III.7 and III.8, are valid for temperatures such that the enumeration functions $\sigma_a$ and $\hat{\sigma}_a$ remain nonnegative.

It is clear from the last two equations that temperature reduction ($\beta$ increase) causes both $\varphi_a$* and $\psi_a$* to drift to lower values, provided that they are still within the limits, III.3 and III.4, respectively. However, such drift must cease when the lower limits are encountered, at which point the system has occupied the lowest available amorphous-state basins. This defines the "ideal glass transition temperature" $T_{ig} \equiv (k_B\beta_{ig})^{-1}$. For isochoric circumstances, this is found from eqs III.3 and III.7 to be

$$k_BT_{ig}(\rho) = \{2[\alpha_0(\rho)\alpha_2(\rho)]^{1/2} - F(\rho)\}^{-1} \quad \text{(III.9)}$$

The isobaric version follows from eqs III.4 and III.8

$$k_BT_{ig}(p) = \{2[\hat{\alpha}_0(p)\hat{\alpha}_2(p)]^{1/2} - \hat{F}(p)\}^{-1} \quad \text{(III.10)}$$

The system remains stuck in the lowest basins at $\varphi_{la}$* or $\psi_{la}$* upon any further cooling below the ideal glass transition temperature.[1,34] This sudden switch from temperature-varying to temperature-invariant $\varphi_a$* or $\psi_a$* is an intrinsic property of the Gaussian landscape distribution model. It should be noted that the ideal glass transition temperature at which the system occupies the lowest-available amorphous-state basin is different from the so-called Kauzmann temperature, where the entropy of the supercooled liquid equals that of the stable crystal.[35]

We close this section III by exhibiting expressions for the heat capacities implied by the Gaussian landscape distribution model. For this model, general expression II.10 for $C_{Va}$ reduces to

$$\frac{C_{Va}}{Nk_B} = -\beta^2 \left\{ \left(\frac{\partial \varphi_a*}{\partial \beta}\right)_\rho + 2\left(\frac{\partial f_1}{\partial \beta}\right)_\rho + \beta\left(\frac{\partial^2 f_1}{\partial \beta^2}\right)_\rho \right\}_{\varphi=\varphi_a*} \quad \text{(III.11)}$$

in which

$$\left(\frac{\partial \varphi_a*}{\partial \beta}\right)_\rho = -\frac{1}{2\alpha_2(\rho)} \quad (0 < \beta < \beta_{ig}(\rho))$$
$$= 0 \quad (\beta_{ig}(\rho) \leq \beta) \quad \text{(III.12)}$$

The parallel result for $C_{pa}$ is

$$\frac{C_{pa}}{Nk_B} = -\beta^2 \left\{ \left(\frac{\partial \psi_a*}{\partial \beta}\right)_p + 2\left(\frac{\partial \hat{f}_1}{\partial \beta}\right)_p + \beta\left(\frac{\partial^2 \hat{f}_1}{\partial \beta^2}\right)_p \right\}_{\psi=\psi_a} \quad \text{(III.13)}$$

in which

$$\left(\frac{\partial \psi_a^*}{\partial \beta}\right)_p = -\frac{1}{\hat{\alpha}_2(p)} \qquad (0 < \beta < \beta_{ig}(p))$$

$$= 0 \qquad (\beta_{ig}(p) \le \beta) \qquad \text{(III.14)}$$

As a consequence of the forms III.5 and III.6 assumed for the vibrational free energies, the heat capacity expressions (eqs III.11 and III.13) now consist of independent configurational and vibrational contributions. It should be noted in passing that these decoupled heat capacity expressions are quite general, given the assumed forms III.5 and III.6; only the specific expressions III.12 and III.14 for $\beta$ derivatives of the dominant depth parameters depend on the Gaussian model choice.

## IV. Aspects of Inherent Structure Enumeration

For simplicity of presentation, we shall confine attention temporarily to the isochoric (constant volume) case. The variational criterion (eq II.9) identifies $\varphi_a^*(\beta, \rho)$ by matching the slopes in $\varphi$ of the curves for $\sigma_a(\varphi)$ and for $\beta\varphi + \beta f_a^{(vib)}(\varphi, \beta, \rho)$. It is easy to see that the prediction of an ideal glass transition at a positive temperature for the Gaussian landscape distribution model stems directly from the fact that its parabolic $\sigma_a(\varphi)$, eq III.1, possesses a positive slope at its lower endpoint, $\varphi_{la}$. That is, $\sigma_a(\varphi)$ for $\varphi \ge \varphi_{la}$ has a Taylor expansion with leading-order term

$$\sigma_a(\varphi) = A(\varphi - \varphi_{la}) + O[(\varphi - \varphi_{la})^2]$$

$$A = \sigma_a'(\varphi_{la} + 0) > 0 \qquad \text{(IV.1)}$$

Indeed, any model landscape distribution possessing this qualitative property can be anticipated to predict a positive-temperature ideal glass transition.

Provided that interest focuses on the immediate neighborhood of the lower limit $\varphi_{la}$, it suffices to disregard the nonlinear terms in expansion (eq IV.1). The number $M(\varphi)$ of distinguishable potential-energy minima (inherent structures) whose energies per particle lie at or below $\varphi > \varphi_{la}$ is expressed by the integral

$$M(\varphi) = C \int_{\varphi_{la}}^{\varphi} \exp[N\sigma_a(\varphi')] \, d\varphi'$$

$$\cong C \int_{\varphi_{la}}^{\varphi} \exp[NA(\varphi' - \varphi_{la})] \, d\varphi'$$

$$= \frac{C}{NA} \{\exp[NA(\varphi - \varphi_{la})] - 1\} \qquad \text{(IV.2)}$$

Inverting this expression leads to the following prediction for the level of system-wide potential-energy excitation below which $M$ distinguishable local minima lie, specifically

$$N[\varphi(M) - \varphi_{la}] = \frac{1}{A} \ln\left(1 + \frac{ANM}{C}\right) \qquad \text{(IV.3)}$$

We now ask how large this last quantity (eq IV.3) must be so that the integer $M$ is some small (but positive and not infinitesimal) fraction of the very large integer $N$

$$M = \xi N \qquad (0 < \xi \ll 1) \qquad \text{(IV.4)}$$

where $\xi$ is independent of $N$. This will be itself a large integer ($M \gg 1$) because we are ultimately interested in the large-system-limit behavior ($N \to \infty$). But because the totality of distinguishable inherent structures is exponentially large in $N$, $M$ is still a miniscule portion of that totality. The choice (eq IV.4) transforms eq IV.3 to

$$N[\varphi(\xi N) - \varphi_{la}] \cong \frac{1}{A} \ln\left(\frac{A\xi N^2}{C}\right)$$

$$= (2/A) \ln N + O(1) \qquad \text{(IV.5)}$$

The implication of eq IV.5 is that the excitation energy above the absolute (amorphous) minimum required to reach the lowest $\xi N$ inherent structures, in a system of $N$ particles, rises logarithmically with $N$. Hence it is unbounded in the large-$N$ limit. This feature appears to violate common qualitative understanding of molecular interactions and of the particle packings that they produce.[28] Starting with a global-minimum amorphous mechanically stable packing, essentially independent local particle rearrangements are possible at a variety of positions throughout the system, the number of which is necessarily proportional to the system's size, i.e., proportional to $N$. These localized rearrangements are not identical in character because they depend on details of particle-packing geometry at each qualifying position within the variable amorphous medium. Such rearrangements consequently will be broadly distributed in excitation energy and will include the well-documented "two-level systems" that appear to be characteristic of most amorphous media.[36,37] However, each typically involves modest displacement of only $O(1)$ particles from their positions at the global minimum, and so each involves only an $O(1)$ excitation energy. Therefore, an $O(1)$ upper limit to excitation energy already includes $O(N)$ distinct local rearrangement possibilities. Consequently, the realistic version of eq IV.5 should have its right member equal to an $N$-independent $O(1)$ quantity, not a logarithmically growing term.

To create a realistic version of eq IV.5, that is to say, one in which the total energy above the deepest amorphous minimum required to reach the lowest $\xi N$ inherent structures ($\xi \ll 1$) is an $O(1)$ quantity, the initial slope of $\sigma_a(\varphi)$ just above $\varphi_{la}$ must be infinite. More specifically, the leading-order behavior for $\varphi > \varphi_{la}$ must have a bounded logarithmic form[28]

$$\sigma_a(\varphi) = -B(\varphi - \varphi_{la}) \ln(\varphi - \varphi_{la}) + O(\varphi - \varphi_{la}) \quad \text{(IV.6)}$$

where $B$ is a positive constant. With this singular form

$$\lim_{\varphi \to \varphi_{la}+0} \left(\frac{d\sigma_a}{d\varphi}\right) = +\infty \qquad \text{(IV.7)}$$

as required, which is not strictly consistent with the presence of a positive-temperature ideal glass transition. Instead of attaining the lower limit value $\varphi_{la}$ at a positive temperature, $\varphi_a^*$ instead continuously drifts downward with decreasing temperature, attaining $\varphi_{la}$ only at absolute zero. However, this observation does not necessarily diminish the utility of the "ideal glass transition" as an empirical device to describe the way in which real glass formers (especially those designated as "fragile"),[38] behave both thermodynamically and kinetically at higher temperature. In connection with simple landscape models such as the Gaussian version described in the previous section III, one needs to bear in mind that expression IV.6 is only a desirable and relevant modification at the low end of the amorphous inherent structure distribution. In any event, it constitutes a feature not directly observable due to the intervention of the laboratory glass transition at a temperature $T_g$, which is always higher than an inferred ideal glass transition temperature.

The argument just presented concerns isochoric (constant volume) conditions. Nevertheless, the reader should be aware that an analogous version applies to isobaric (constant pressure)
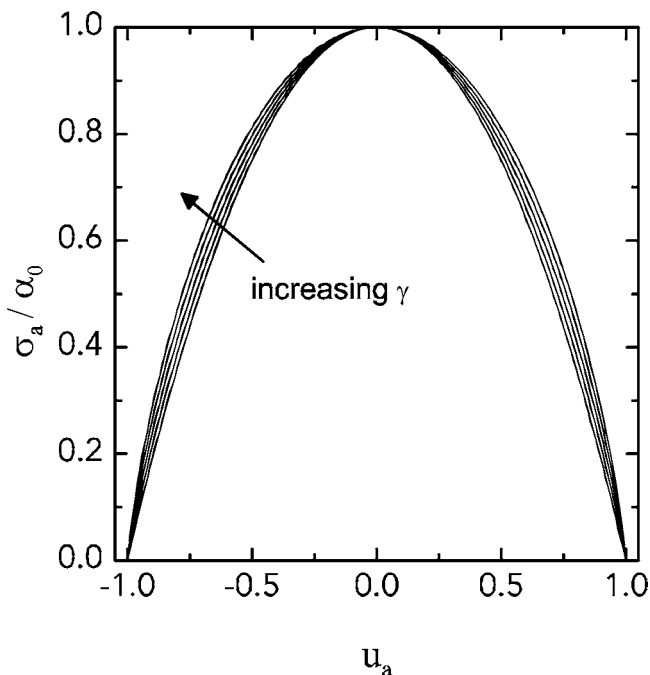
**Figure 1.** Plots of the scaled enumeration function $\sigma_a/\alpha_0$ for the logarithmically perturbed Gaussian model. The independent variable is the scaled isochoric depth parameter, defined in eq V.2. The curves shown correspond to five choices for the interpolation parameter $\gamma = 0.00, 0.25, 0.50, 0.75,$ and $1.00$. The unperturbed Gaussian model arises from the first of these, $\gamma = 0$.

circumstances, in which the intensive potential-enthalpy order parameter $\psi$ replaces the intensive potential-energy order parameter $\varphi$. The corresponding conclusion is that isobaric landscape enumeration models with finite positive initial slopes $\hat{\sigma}_a{}'(\psi_{la} + 0)$ are also at variance with qualitative understanding of intermolecular interactions in condensed media. Consequently, isobaric enumeration functions also require a bounded logarithmic form analogous to that shown in eq IV.6 above.

## V. Logarithmic Modification

The concepts presented in the preceding section IV warrant examination of a modified version of the simple Gaussian model that was discussed in section III. Specifically, it is important to incorporate the infinite-slope logarithmic form (eq IV.6) at the lower endpoint of the enumeration intervals of $\sigma_a$ and $\hat{\sigma}_a$ in order to avoid the misleading implication of a positive-temperature ideal glass transition. So as to change the original model as little as possible, we have chosen to retain its bilateral symmetry about its maximum.

When it is expressed in reduced form, the isochoric Gaussian model has the following appearance

$$\sigma_a/\alpha_0 = 1 - u^2 \tag{V.1}$$

where the scaled energy order parameter is defined by

$$u = \frac{\varphi - \varphi_0}{\varphi_0 - \varphi_{la}} \qquad (-1 \le u \le 1) \tag{V.2}$$

The modification now to be considered incorporates a nonnegative parameter $\gamma$ into a generalization of the scaled form (V.1)

$$\sigma_a/\alpha_0 =$$
$$(1 - \gamma)(1 - u^2) + \gamma\{1 - (2\ln 2)^{-1}[(1 + u)\ln(1 + u) + (1 - u)\ln(1 - u)]\} \tag{V.3}$$

By increasing $\gamma$ continuously over the interval $0 \le \gamma \le 1$, this expression transforms continuously from the original Gaussian model, eq V.1, to a pure logarithmic form. Regardless of the $\gamma$ value in this interval, $\sigma_a/\alpha_0$ vanishes at $u = \pm 1$ and passes through a single maximum at $u = 0$, for which $\sigma_a/\alpha_0 = 1$.

Figure 1 presents plots of the logarithmically modified function (eq V.3) for several $\gamma$ choices that span its interval of positive values. An obvious feature presented by that group of curves is that rather little overall change in shape results as $\gamma$ increases to switch the model from pure Gaussian form to pure logarithmic form. Consequently, this modification should not materially compromise the ability to represent many-body thermal behavior as has been claimed for the unmodified Gaussian model. The infinite slopes that exist at the endpoints with positive $\gamma$ are subtle and barely visible in Figure 1 but remain significant features that frustrate the occurrence of ideal glass transitions.

We shall continue to suppose that the vibrational free energy function $f_a^{(\mathrm{vib})}$ is adequately represented by eq III.5. Upon inserting the logarithmically modified model function (eq V.3) and the vibrational free-energy function (eq III.5) into criterion II.9, an implicit result emerges for determination of the scaled order parameter $u_a{}^*$ as a function of temperature

$$-\left[2(1 - \gamma)u_a{}^* + \frac{\gamma}{2\ln 2}\ln\left(\frac{1 + u_a{}^*}{1 - u_a{}^*}\right)\right] = \left(\frac{\varphi_0 - \varphi_{la}}{\alpha_0}\right)[\beta + F(\rho)] \tag{V.4}$$

This result displays a notable characteristic that arises from the second factor in the right member. Specifically, the basin-depth dependence of vibrational free energy embodied by the function $F(\rho)$ creates an effective shift in the inverse-temperature quantity $\beta$

$$\beta + F(\rho) = \beta_{\mathrm{eff}} = (k_B T_{\mathrm{eff}})^{-1} \tag{V.5}$$

Referring to eq III.11, one sees that the configurational contribution to the isochoric heat capacity is

$$\frac{C_{V_a}{}^{(\mathrm{conf})}}{Nk_B} = -\beta^2(\varphi_0 - \varphi_{la})\left(\frac{\partial u_a{}^*}{\partial \beta}\right)_\rho \tag{V.6}$$

By applying a $\beta$ derivative to eq V.4, this converts to a form specific to the logarithmically modified Gaussian model

$$\frac{C_{V_a}{}^{(\mathrm{conf})}}{Nk_B} = \frac{\beta^2(\varphi_0 - \varphi_{la})^2}{\alpha_0}\left[2(1 - \gamma) + \left(\frac{\gamma}{\ln 2}\right)\left(\frac{1}{1 - (u_a{}^*)^2}\right)\right]^{-1} \tag{V.7}$$

Each of the isochoric results shown in eqs V.1−V.7 has an analogous isobaric partner of exactly the same formal structure. Because of the strong correspondence, it should not be necessary to repeat the sequence of equations. One point may be worth stressing, however. The available evidence from isochoric computer simulations[32,33] indicates that the vibrational quantity $F(\rho)$ is positive, implying that the more disordered (and thus higher-energy) inherent structures are more tightly packed and more vibrationally constrained. By contrast, isobaric conditions should relieve that tighter packing and consequent vibration-constraining effect,[39] possibly leading in some cases to a negative $\hat{F}(p)$. If that is so, isochoric and isobaric conditions
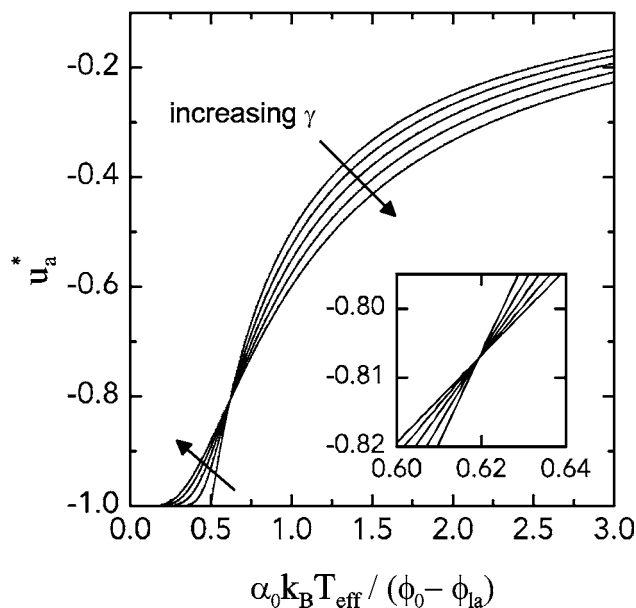
**Figure 2.** Curves of the equilibrium scaled isochoric depth parameter $u_a^*$ vs effective temperature. The same five $\gamma$ values (0.00, 0.25, 0.50, 0.75, and 1.00) have been used here as in Figure 1. As remarked in the text, these results are immediately applicable to isobaric conditions, upon reinterpretation of the axis labels.

would lead respectively to opposing shifts of the effective inverse temperature compared to absolute temperature.

## VI. Numerical Results

Figure 2 presents the results of numerical calculations for the scaled isochoric depth parameter $u_a^*$, based on eq V.4, plotted vs the scaled effective temperature

$$\frac{\alpha_0 k_B T_{eff}}{\varphi_0 - \varphi_{la}} \equiv \left(\frac{\alpha_0}{\varphi_0 - \varphi_{la}}\right)\left(\frac{k_B T}{1 + F(\rho)k_B T}\right) \qquad \text{(VI.1)}$$

The curves shown involve the same five $\gamma$ choices that were used in Figure 1. Figure 2 is also immediately relevant to the isobaric case, provided that the vertical axis represents scaled potential-enthalpy depth parameter $\hat{u}_a^*$ and the horizontal axis represents the corresponding effective temperature

$$\frac{\hat{\alpha}_0 k_B \hat{T}_{eff}}{\psi_0 - \psi_{la}} = \left(\frac{\hat{\alpha}_0}{\psi_0 - \psi_{la}}\right)\left(\frac{k_B T}{1 + \hat{F}(p)k_B T}\right) \qquad \text{(VI.2)}$$

Notice that as $T \rightarrow \infty$, the isochoric effective temperature $T_{eff} \rightarrow [k_B F(\rho)]^{-1}$ while the isobaric effective temperature $\hat{T}_{eff} \rightarrow [k_B \hat{F}(p)]^{-1}$. As indicated previously, under some circumstances it is possible that these limits could have opposing signs.

Two notable features stand out in Figure 2. First, in distinction to the $\gamma = 0$ Gaussian model limit, the $u_a^*$ (or $\hat{u}_a^*$) curves for $\gamma > 0$ only fall to zero when the effective temperature itself falls to zero. As expected, therefore, the logarithmic modification formally eliminates the ideal glass transition. Second, the numerical results shown seem to suggest that the entire family of curves for $0 \leq \gamma \leq 1$ all pass through a common fixed point. The insert in Figure 2 strengthens that conclusion by presenting a magnified view of the common crossing region.

It is possible to demonstrate directly that indeed there is a mathematically well-defined common crossing point in Figure 2. This point can be located by differentiating eq V.4 with respect to the mixing coefficient $\gamma$, solving for $du_a^*/d\gamma$ and setting that derivative equal to zero. The result is a transcen-
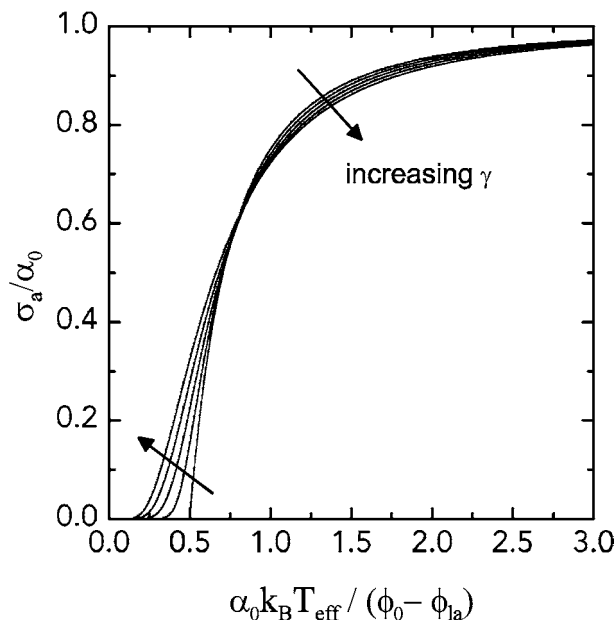


**Figure 3.** Variation of the scaled isochoric enumeration function $\sigma_a/\alpha_0$ with scaled effective temperature. As in the preceding Figures 1 and 2, the values of the mixing parameter $\gamma$ are 0.00, 0.25, 0.50, 0.75, and 1.00.

dental equation

$$u_a^* = \frac{2^{4u_a^*} - 1}{2^{4u_a^*} + 1} \qquad \text{(VI.3)}$$

Its relevant real root is found to be

$$u_a^* \cong -0.8072515584 \qquad \text{(VI.4)}$$

By substituting this value into eq V.4, one evaluates the effective temperature at this fixed point

$$\frac{\alpha_0 k_B T_{eff}}{\varphi_0 - \varphi_{la}} = -\frac{1}{2u_a^*}$$

$$\cong 0.6193856113 \qquad \text{(VI.5)}$$

It can be shown that a fixed point exists whenever two basin enumeration functions $H(u)$ and $G(u)$ are combined linearly (e.g., $\sigma_a/\alpha_0 = (1 - \gamma) H(u) + \gamma G(u)$, as shown in eq V.3 for the Gaussian and logarithmic cases), provided a slope-matching condition $dH/du = dG/du$ is satisfied for some particular value $u^*$ of $u$. In such cases, the slope at the invariant point is a measure of the relative weight of each basin enumeration function; the higher the slope, the more a real system's depth distribution of basins approximates that described by the function $H(u)$.

Figure 3 shows the variation of the scaled enumeration function $\sigma_a/\alpha_0$ with the scaled isochoric effective temperature. The same five $\gamma$ values that were used in the preceding Figures 1 and 2 are represented in this plot as well. Although a quick glance at Figure 3 might suggest the presence of another fixed crossing point, that is actually not the case.

Figure 4 offers plots of configurational heat capacities for the same $\gamma$ choices as in the previous plots. These curves are based on the earlier eq V.7. It is very clear that continuously turning on the logarithmic perturbation diminishes the heat capacity at low temperature while still producing a maximum in this quantity.
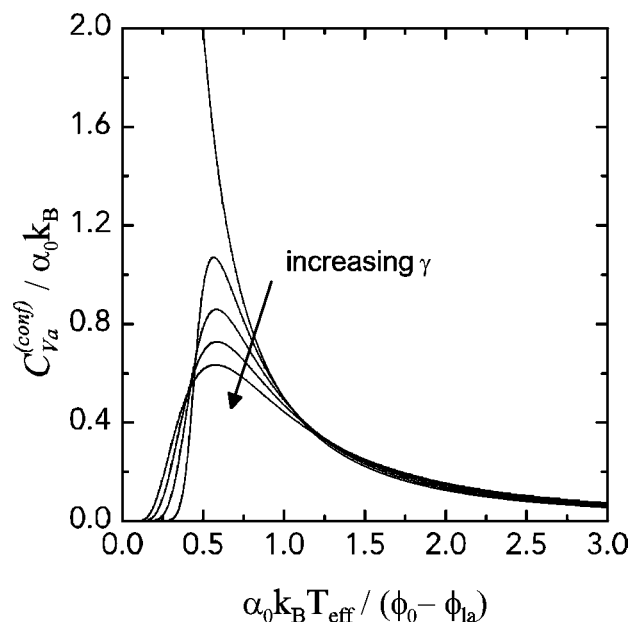
Model Energy Landscapes

*J. Phys. Chem. B, Vol. 107, No. 51, 2003* **14441**



**Figure 4.** Scaled values of the isochoric configurational heat capacity for the logarithmically modified Gaussian model. The values of the mixing parameter $\gamma$ are the same as in the preceding Figures.

Although the logarithmic modification formally eliminates an ideal glass transition, the thermodynamic properties produced by the model, when examined only above a kinetic glass transition, might reasonably be extrapolated to predict an ideal glass transition at positive temperature. One such extrapolation might utilize the inflection point of $\sigma_a(\varphi_a{}^*)$ or $\hat{\sigma}_a(\psi_a{}^*)$ vs temperature and linearly extrapolate the slope at the inflection point to intersection with the horizontal axis. This predicts an apparent ideal glass transition temperature for isochoric conditions

$$T_{ig}(\text{apparent}) = T_{infl} - \frac{\sigma_a(T_{infl})}{\sigma_a{}'(T_{infl})} \qquad (VI.6)$$

with an equivalent expression for isobaric conditions. Figure 5 provides a scaled plot of the apparent ideal glass transition temperature estimated in this way. Notice that the effect of increasing $\gamma$ from 0 to 1 is to reduce the apparent ideal glass transition temperature by a factor of approximately 2.

## VII. Conclusions and Discussion

The principal conclusion to be drawn from this paper is that while simple models of the Gaussian type for enumeration of inherent structures offer a crude but useful approximation, they require modification at the lower end of their distributions. This modification is necessary to avoid spurious prediction of an ideal glass transition. Careful examination of the enumeration problem for atomic and molecular glass formers, whether they are subject to isochoric (constant volume) or isobaric (constant pressure) conditions, implies that logarithmic corrections are necessary. A specific modification of the Gaussian model conforming to this necessity has been proposed here, and has been the object of numerical study.

The logarithmically modified Gaussian model presents considerable flexibility for representing either experimental of simulational data for real or computational glass formers, respectively. In the isochoric setting, the adjustable parameters are $\alpha_0$, $\alpha_2$, $\varphi_0$, $f_1(\beta)$, $F$, and the logarithmic mixing parameter $\gamma$. Isobaric conditions present an equivalent set. On account of
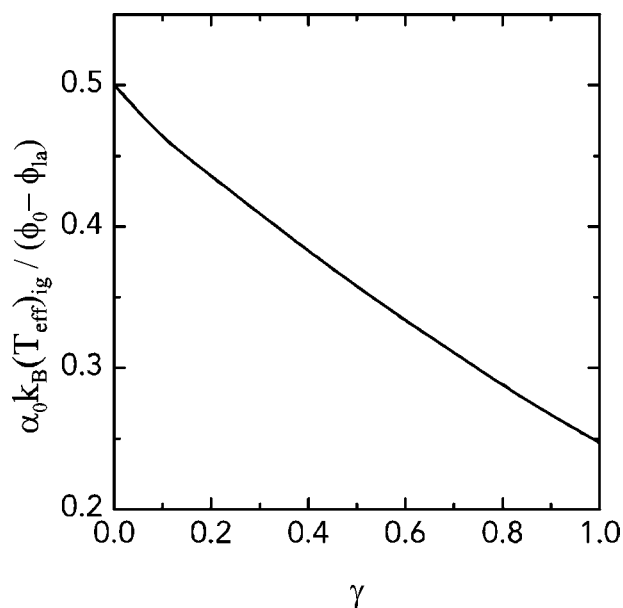


**Figure 5.** Apparent ideal glass transition effective temperatures (scaled) for the logarithmically modified Gaussian model as a function of the mixing parameter $\gamma$. These temperatures arise from an inflection-point extrapolation criterion, eq VI.6.

this flexibility, attempts to determine optimal-fit values for these parameters from standard calorimetric data alone may not yield unique results. It may be necessary to supplement that data with experimental hyperquenching results[39] or simulational sampling of inherent structures and evaluation of their basin properties.[32,33] It would also be valuable to investigate the theoretical possibility to carry out the enumeration program outlined in Section IV above for the low end of the potential-energy or potential-enthalpy range in order to assign the logarithmic parameter $\gamma$ directly.

Although the Adam−Gibbs relation, eqs II.15−II.17, connects calorimetric behavior of glass formers to their kinetic characteristics and in particular makes that connection for the logarithmically modified Gaussian model, its fundamental "landscape" justification remains somewhat obscure. It has been pointed out[40] that from the purely mathematical point of view, any given basin-depth distribution can correspond to a wide range of potential-energy or potential-enthalpy multidimensional topographies. In particular, this means that the depth distribution by itself does not control the arrangement or height of barriers separating distinct inherent structures and their basins. Therefore, the empirical success of the Adam−Gibbs relation implies the presence and kinetic relevance of a physical constraint on multidimensional "landscapes" that severely limits those that satisfy the depth distribution alone. An attractive possibility that deserves future research attention is that physically reasonable landscapes obey a topographic scaling relation that links basin populations at a given depth to the average barrier heights (landscape "roughness") at that depth.

The model enumeration function described in this paper has some obvious limitations. One of these is its underlying assumption of bilateral symmetry about its maximum, introduced here for simplicity and on account of no compelling evidence to the contrary. Another limitation concerns the elementary form adopted for the isochoric and isobaric vibrational free energy functions, eqs III.5 and III.6; recall that these assumed forms had the effect of decoupling configurational and vibrational degrees of freedom in the total free energy, as well as leading to the existence of an effective temperature, eq V.5. Finally, it should be stressed that the model investigated here does not

produce any phase transitions within the amorphous manifold of basins. For that reason, it is inapplicable to those substances such as carbon,[41] phosphorus,[42] silica,[43] and water[44] for which liquid−liquid phase transitions have been reported. As a result of these considerations, a case can be made for various extensions of the present work, but for any extension it remains necessary to observe the low-end enumeration condition advanced above in Section IV.

## References and Notes

(1) Debenedetti, P. G.; Stillinger, F. H. *Nature* **2001**, *410*, 259.
(2) Ediger, M. D.; Angell, C. A.; Nagel, S. R. *J. Phys. Chem.* **1996**, *100*, 13200.
(3) Mézard, M.; Parisi, G. *Phys. Rev. Lett.* **1999**, *82*, 747.
(4) Speedy, R. J. *J. Phys. Chem. B* **1999**, *103*, 4060.
(5) Crowe, J. H.; Carpenter, J. F.; Crowe, L. M. *Annu. Rev. Physiol.* **1998**, *60*, 73.
(6) Greer, A. L. *Science* **1995**, *267*, 1947.
(7) Hodge, I. M. *Science* **1995**, *267*, 1945.
(8) Doremus, R. H. *Glass Science*, 2nd ed.; Wiley: New York, 1994.
(9) Angell, C. A.; Ngai, K. L.; McKenna, G. B.; McMillan, P. F.; Martin, S. W. *J. Appl. Phys.* **2000**, *83*, 3113.
(10) Anderson, P. W. *Science* **1995**, *267*, 1615.
(11) Stillinger, F. H.; Weber, T. A. *Phys. Rev. A* **1982**, *25*, 978.
(12) Sastry, S.; Debenedetti, P. G.; Stillinger, F. H. *Nature* **1998**, *393*, 554.
(13) Utz, M.; Debenedetti, P. G.; Stillinger, F. H. *J. Chem. Phys.* **2001**, *114*, 10049.
(14) Schulz, M. *Phys. Rev. B* **1998**, *57*, 11319.
(15) Malandro, D. L.; Lacks, D. J. *Phys. Rev. Lett.* **1998**, *81*, 5576.

(16) Scala, A.; Starr, F. W.; La Nave, E.; Sciortino, F.; Stanley, H. E. *Nature*, **2000**, *406*, 166.
(17) Stillinger, F. H. *Phys. Rev. E* **1999**, *59*, 48.
(18) Hardin, C.; Eastwood, M. P.; Prentiss, M.; Luthey-Schulten, Z.; Wolynes, P. G. *J. Comput. Chem.* **2002**, *23*, 138.
(19) Jónsson, H.; Andersen, H. C. *Phys. Rev. Lett.* **1988**, *60*, 2295.
(20) Sciortino, F.; Kob, W.; Tartaglia, P. *Phys. Rev. Lett.* **1999**, *83*, 3214.
(21) Büchner, S.; Heuer, A. *Phys. Rev. Lett.* **2000**, *84*, 2168.
(22) Heuer, A.; Büchner, S. *J. Phys.: Condens. Matter* **2000**, *12*, 6535.
(23) Angelani, L.; Di Leonardo, R.; Ruocco, G.; Scala, A.; Sciortino, F. *Phys. Rev. Lett.* **2000**, *85*, 5356.
(24) Broderix, K.; Bhattacharya, K. L.; Cavagna, A.; Zippelius, A.; Giardina, I. *Phys. Rev. Lett.* **2000**, 85, 5360.
(25) Sastry, S. *Nature* **2001**, *409*, 164.
(26) Saika-Voivod, I.; Poole, P. H.; Sciortino, F. *Nature* **2001**, *412*, 514.
(27) Götze, W.; Sjögren, L. *Rep. Prog. Phys.* **1992**, *55*, 241.
(28) Stillinger, F. H. *J. Chem. Phys.* **1988**, *88*, 7818.
(29) Stillinger, F. H. *J. Phys. Chem. B* **1998**, *102*, 2807.
(30) Adam, G.; Gibbs, J. H. *J. Chem. Phys.* **1965**, *43*, 139.
(31) Debenedetti, P. G.; Truskett, T. M.; Lewis, C. P.; Stillinger, F. H. *Adv. Chem. Eng.* **2001**, *28*, 21.
(32) Sastry, S. *Nature* **2001,** *409*, 164.
(33) La Nave, E.; Mossa, S.; Sciortino, F. *Phys. Rev. Lett.* **2002**, *88*, 225701.
(34) Gibbs, J. H.; DiMarzio, E. A. *J. Chem. Phys.* **1958**, *28*, 373.
(35) Kauzmann, W. *Chem. Rev.* **1948**, *43*, 219.
(36) Anderson, P. W.; Halperin, B. I.; Varma, C. M. *Philos. Mag.* **1972**, *25*, 1.
(37) *Amorphous Solids: Low-Temperature Properties*; Phillips, W. A., Ed.; Springer: New York, 1972.
(38) Angell, C.A. *Science* **1995**, *267*, 1924.
(39) Angell, C. A.; Yue, Y.; Wang, L.-M.; Copley, J. R. D.; Borick, S.; Mossa, S. *J. Phys.: Condens. Matter* **2003**, *15*, S1051.
(40) Stillinger, F. H.; Debenedetti, P. G. *J. Chem. Phys.* **2002**, *116*, 3353.
(41) van Thiel, M.; Ree, F. H. *Phys. Rev. B* **1993**, *48*, 3591.
(42) Katayama, Y.; Mizutani, T.; Utsumi, W.; Shimomura, O.; Yamakata, M.; Funakoshi, K. *Nature* **2000**, *403*, 170.
(43) Lacks, D. J. *Phys. Rev. Lett.* **2000**, *84*, 4629.
(44) Mishima, O. *Phys. Rev. Lett.* **2000**, *85*, 334.